

RESEARCH

Open Access



# Immune-mediated mechanisms in acute osteofascial compartment syndrome: insights from multi-omics analysis

Qinzhen Lu<sup>1†</sup>, He Ling<sup>1†</sup>, Yonghui Lao<sup>1</sup>, Junjie Liu<sup>1</sup>, Wei Su<sup>1</sup> and Zhao Huang<sup>1\*</sup>

## Abstract

**Background** Acute Osteofascial Compartment Syndrome (AOCS) stands as a critical surgical emergency, often secondary to various diseases. Its clinical manifestation arises from increased pressure within the fascial compartment, resulting in diminished tissue perfusion and consequential ischemic damage. Presently, clinical diagnostics lack effective biological markers, and patients face a grim prognosis, experiencing muscle contractures, necrosis, amputations, renal failure, and even mortality. The primary treatment, fasciotomy, poses infection risks and potential nerve damage. Hence, there is an urgent need for research elucidating AOCS's pathogenic mechanism and exploring novel treatments.

**Methods** To address this, we established a rat model of AOCS, extracting toe flexor muscles from both experimental and control groups. Employing second-generation high-throughput sequencing, we obtained comprehensive mRNA, lncRNA, circRNA, and miRNA data. Comparative analysis of expression differences between AOCS and control groups, followed by in-depth examination, allowed us to unravel the intricacies of AOCS occurrence from a multi-omics perspective.

**Results** Our research findings indicate that AOCS is an immune-mediated inflammatory disease, primarily involving immune cells, especially neutrophils. In addition, genes associated with ferroptosis, a form of regulated cell death, are found to be upregulated in the rat model, with non-coding RNAs playing a role in regulatory interactions.

**Conclusions** These results suggest that neutrophils may undergo ferroptosis, thereby enhancing inflammation and immune responses in the fascial compartment, which promotes disease progression. Furthermore, these findings reveal the interactions between immune molecules and pathways in AOCS, which are significant for a deeper understanding of the pathogenesis of the disease and the development of targeted therapeutic strategies.

**Keywords** Acute osteofascial compartment syndrome, Ischemic damage, High-throughput sequencing, Ferroptosis, CGAS–STING

## Introduction

Acute osteofascial compartment syndrome (AOCS) is a surgical emergency that can arise as a secondary condition to various diseases. It manifests as increased pressure within the fascial compartment, leading to decreased tissue perfusion and resulting in ischemic damage to the fascial compartment tissues [1]. The most common primary cause of acute lower limb osteofascial compartment syndrome is traumatic fractures, followed

<sup>†</sup>Qinzhen Lu and He Ling have contributed equally to this work.

\*Correspondence:  
Zhao Huang  
65613689@qq.com

<sup>1</sup> Department of Orthopedics Trauma and Hand Surgery, The First Affiliated Hospital of Guangxi Medical University, NO. 6 Shuang Yong Road, Nanning 530022, Guangxi, China



by non-fracture soft tissue injuries and vascular-related diseases [1–4].

Despite nearly 130 years of research on acute lower limb osteofascial compartment syndrome, its diagnosis remains a significant challenge [1]. Currently, there is a lack of effective biological diagnostic markers in clinical practice. The clinical prognosis is unfavorable, with patients often experiencing muscle contractures, necrosis, amputations, renal failure, and even death [1, 5]. The main treatment for acute lower limb osteofascial compartment syndrome is fasciotomy to alleviate the high pressure within the fascial compartment. However, for late-stage AOCS patients, fasciotomy may increase the risk of infections [6]. In addition, nerve damage is a common complication of fasciotomy treatment [7]. The diagnostic and therapeutic methods for AOCS are limited and challenging to meet clinical needs. Therefore, there is an urgent need for in-depth research on the pathogenic mechanisms and new therapeutic targets for AOCS.

One of the pathological mechanisms of acute lower limb osteofascial compartment syndrome is ischemia and reperfusion injury (IRI) [1]. Abnormal skeletal muscle metabolism is a crucial early event in AOCS injury [8]. Studies have shown that improving tissue metabolism can effectively alleviate skeletal muscle ischemia–reperfusion injury, increase muscle tension, and reduce the production of oxidative stress and inflammatory factors [9]. However, there is currently a lack of specific drugs for the treatment of acute lower limb osteofascial compartment syndrome. With a wealth of genomic information accumulating in the era of "big data" in biomedical research [10, 11], we established a rat model of AOCS. We extracted the toe flexor muscles from the experimental and control groups of rat hind legs, performed second-generation high-throughput sequencing, obtained mRNA, lncRNA, circRNA, and miRNA sequencing data, compared the expression differences between AOCS and control groups, and conducted in-depth analysis to unravel the occurrence process of AOCS from a multi-omics perspective. In this process, the potential role of the cGAS–STING pathway is particularly noteworthy. Literature reports indicate that the cGAS–STING pathway plays a critical role in sensing intracellular DNA damage and maintaining immune homeostasis [12]. Meanwhile, the cGAS–STING pathway also participates in immune response modulation in inflammatory diseases [13, 14], especially in response to cellular damage, self-DNA leakage, or pathogen infection. Ischemia–reperfusion injury leads to cellular damage and death, releasing a large amount of intracellular DNA. These DNA fragments may activate the cGAS–STING pathway and further modulate immune responses and inflammatory reactions. Therefore, researching the role of

the cGAS–STING pathway in AOCS not only aids in a deeper understanding of its pathological mechanisms but may also offer new insights for the development of targeted therapeutic strategies. This is especially relevant in seeking potential targets to alleviate skeletal muscle ischemia–reperfusion injury, reduce oxidative stress, and decrease the production of inflammatory factors.

## Materials and methods

### Experimental design flowchart

The experimental design of this study is summarized in the flowchart (Fig. 1).

### Establishment of animal model

#### *Acute osteofascial compartment syndrome (AOCS) animal model, including: ligation section and monitoring section*

The ligation section includes: cotton thread and vascular forceps. The cotton thread is used to tie the base of the rat's thigh, and vascular forceps assist in securing the knot during ligation. The monitoring section includes: scalp needle (size 8#), disposable infusion set, saline (100 mL/bottle), disposable pressure sensor (PX2600YZB/USA 3717-2015), electrocardiogram (ECG) monitor (e.g., Mindray 115–021306-00/PHILIPS). The

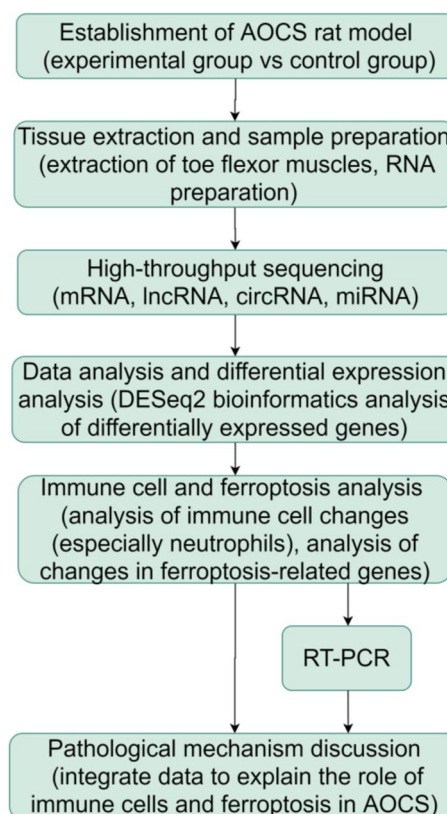


**Fig. 1** Experimental design flowchart

scalp needle is connected to saline via a disposable infusion set, then linked to the pressure transducer through a three-way connector. The pressure transducer is connected to the ECG monitor, which reads ICP and diastolic blood pressure (DBP).  $\Delta p$  ( $\Delta p = \text{DBP} - \text{ICP}$ ) can be calculated accordingly (Fig. 2).

**Procedure for establishing the acute osteofascial compartment syndrome model:**

- a. 400–500 g SD rats were fasted for 12 h before the experiment, with free access to water.
- b. During the experiment, rats were weighed, and intraperitoneal injection of chloral hydrate anesthesia was administered. The concentration of chloral hydrate was 10%, and the dosage was 30–50 mg/kg to maintain anesthesia throughout the experiment.
- c. Measure the circumference C1 of the knee joint at the base of the thigh using a soft ruler. Use cotton thread to tie the thigh near the base to block blood flow to the lower limbs. Assist in securing the knot with vascular forceps, ensuring that the circumference of the thigh base after ligation is  $C2 = C1 \times 1/2$ .
- d. Specific steps for measuring  $\Delta p$  are as follows:

① Shave the hair on the lower limbs of the rat. After routine disinfection, take a point 1 cm above the ankle joint of the rat as the puncture site. Perform a 45° angle puncture and measure the pressure using the vertical pressure measurement method until the

water column is balanced and temporarily close the water column through the three-way connector.

② Connect the vertical water column pressure measurement device to the pressure transducer through a three-way connector. Connect the pressure transducer to the ECG monitor using the ECG monitor cable. Place the pressure transducer at the same level as the limb to be measured and zero it.

③ Open the three-way connector to connect the vertical water column to the pressure transducer. Read ICP through the ECG monitor.

④ Use a indwelling needle for carotid artery puncture, insert an infusion tube into the carotid artery, and monitor DBP using the same method.

⑤ Calculate  $\Delta p$ .

Observe for 12 h; if during this period  $\Delta p < 30$  mmHg and the duration is  $> 2$  h, consider the model established successfully, confirming the occurrence of Acute Compartment Syndrome (AOCS) [15, 16]. If  $\Delta p$  is still not  $< 30$  mmHg after 12 h, perform a second ligation at the same location as the first ligation, making the post-ligation thigh base circumference  $C3 = C1 \times 1/2$ . Continue monitoring until  $\Delta p < 30$  mmHg, and the duration is  $> 2$  h.

1. Rat
2. Indwelling needle and infusion tube
3. Ligation site at the base of the thigh
4. Scalp needle
5. Disposable infusion set

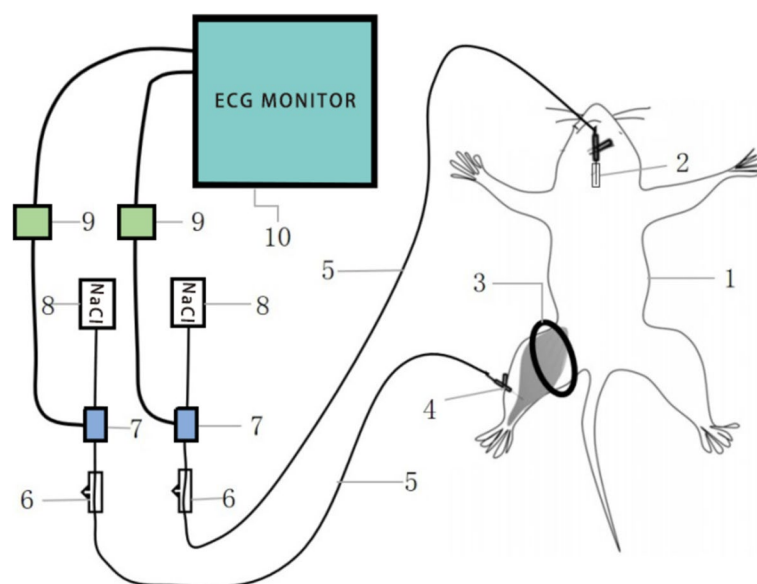


**Fig. 2** Schematic diagram of the animal model structure

6. Three-way connector
7. Pressure transducer
8. Saline solution
9. ECG monitor cable
10. ECG monitor

### Experimental grouping

The experiment is divided into two groups: the experimental group and the control group. The experimental group undergoes modeling treatment, while the control group receives no treatment.

### Sequencing analysis

Three rats are included in each of the experimental and control groups. When the  $\Delta p$  of rats in the experimental group is  $< 30$  mmHg, and the duration is  $> 2$  h, diagnosing the occurrence of Acute Compartment Syndrome (AOCS) indicates successful modeling. Toe flexor muscles from the rat hind legs are collected for second-generation high-throughput sequencing. Total RNA is extracted using the miRNeasy Mini Kit (Germany). cDNA library construction and sequencing are performed using the Illumina HiSeq2000 sequencer at a biotechnology company in Shanghai, China. The raw sequencing reads are mapped to the Sscrofa11.1 reference genome. Transcript expression is quantified in Fragments Per Kilobase of exon model per Million mapped reads (FPKM). Differential gene expression levels are identified using EdgeR [17]. The  $q$  value BioConductor package is utilized to adjust  $P$  values for differential gene expression by controlling the False Discovery Rate (FDR). Genes with  $q \leq 0.05$  and a fold change  $\geq 2$  are defined as differentially expressed genes (DEGs). The ClusterProfiler R package is employed for GO functional enrichment analysis and KEGG pathway enrichment analysis of DEGs. Entries with  $q \leq 0.05$  are considered significantly enriched.

### Protein-protein interaction (PPI) network analysis

The STRING online tool (<https://string-db.org/cgi/input.pl>) is used to construct a DEGs PPI network with a confidence score  $> 0.4$  [18, 19]. Subsequently, data on the HO-1 gene and its associated genes are imported into Cytoscape (version 3.6.0, <http://chianti.ucsd.edu/cytoscape-3.6.0/>) for analyzing the interaction relationships among genes, as well as the proteins they encode, and for visualization.

### Clustering algorithm

Unsupervised consensus clustering is performed on the prognosis NRG ( $p < 0.05$ ) expression profiles using the "ConsensusClusterPlus" package. The optimal number

of clusters is determined based on cumulative distribution curves and K-means. Principal Component Analysis (PCA) confirms the effectiveness of the clustering.

### Pathway enrichment analysis

The "limma" package ( $FDR < 0.05$ ,  $\log_2(FC) > 1$ ) is utilized to detect differentially expressed genes (DEGs) between high and low-risk groups. Subsequently, using "c2.cp.kegg.v7.4.symbols.gmt" as the default gene set, the "clusterProfiler" package is employed for Gene Set Enrichment Analysis (GSEA) and Gene Ontology (GO) enrichment analysis of different risk groups. In addition, "h.all.v7.5.1.symbols.gmt" serves as the default gene set for Gene Set Variation Analysis (GSVA) using the "GSVA" package, exploring heterogeneity in various biological processes. The  $t$  value indicates differences in pathway activity between high-risk and low-risk groups. The results of the enrichment analysis are visualized using the "ggplot2" and "GseaVis" packages.

### RT-PCR

Total RNA was extracted from skeletal muscle tissue using the TRIzol RNA extraction kit (Bioengine, Shanghai, China). The concentration and purity of the RNA were determined using a NanoDrop spectrophotometer (Thermo Fisher Scientific, USA). cDNA was synthesized from the extracted RNA using a reverse transcription kit (Bioengine, Shanghai, China). PCR amplification was performed on the Applied Biosystems QuantStudio 3&5 Real-Time PCR System (Thermo Fisher Scientific, USA) to detect the mRNA levels of relevant genes, including Gpx4, Edn1, Egr1, Il1b, Hp, Junb, Jund, Nos2, Nod2, Homx1, Slc39a14, Ptpcr, Nfkbiz, IL33, Cxcl1, and Cxcr2, with  $\beta$ -actin serving as the internal control for normalization. The relative expression levels were calculated using the  $2^{-\Delta\Delta CT}$  method. The qRT-PCR reaction conditions were as follows: an initial denaturation at 95 °C for 3 min, followed by 40 cycles of 95 °C for 5 s and 60 °C for 20 s. The primers for each gene were synthesized by Sangon Biotech (Shanghai, China), and their sequences are listed below: Nod2, forward, 5'-GCTCAGTCTCGCTTCCTCAGTAC-3'; reverse, 5'-CCGCAGCTCTAAGGTGTTCTCC-3'; Cxcr2, forward, 5'-TGGTCC TCGTCTTCCTGCTCTG-3'; reverse, 5'-CGTTCTGGC GTTCACAGGTCTC-3'; Cxcl1, forward, 5'-GCAGACAGT GGCAGGGATTAC-3'; reverse, 5'-TGAGTGTGGCTA TGACTTCGGTTTG-3'; IL33, forward, 5'-GCGTTTGCT GCATCAGTTGACAC-3'; reverse, 5'-AGATTGGTCGTT GTATGTGCTCAGG-3'; Nfkbiz, forward, 5'-GATCGT GGACAAGCTGCTGGAC-3'; reverse, 5'-AGGCCAGGC TCCGTAGAAGTAAG-3'; Ptpcr, forward, 5'-GGCAAG GAACAACCGACGATGG-3'; reverse, 5'-CTTGGCTGC TGAGTGTCTGAGTG-3'; Gpx4, forward, 5'-AGGCAG GAGCCAGGAAGTAATC-3'; reverse, 5'-ACCACGCAG

CCGTTCTTATC-3'; Hmox1, forward, 5'-GGGTCAGGTGTCCAGGGAAGG-3'; reverse, 5'-TGGGTTCTGCTTGTTTCGCTCTATC-3'; Slc39a14, forward, 5'-TGTGTCTGTCTTCCAAGGCATTAGC-3'; reverse, 5'-ACCAGCATTGAGCAGGATAACGAAG-3'; Nos2, forward, 5'-TCTTGGAGCGAGTTGTGGATTGTTTC-3'; reverse, 5'-AGTGATGTCCAGGAAGTAGGTGAGG-3'; Junb, forward, 5'-CGGATCTTGGGCTGCTCAAACCTC-3'; reverse, 5'-TCGGCGAACTCTGCTCCTC-3'; Junb, forward, 5'-ACAAACTCC TGAAACCCACCTTAGC-3'; reverse, 5'-CCTGCCCACTGCCCTCTG-3'; Hp, forward, 5'-ACAGTGAGAATGCGACAGCCAAG-3'; reverse, 5'-TCAGCCCGATATCCA CCACAGAG-3'; Egr1, forward, 5'-GCCAGGAGTGATGAACGCAAGAG-3'; reverse, 5'-GGATGGGTAGGAAGAGAGGGAAGAG-3'; Edn1, forward, 5'-CTTCTGCCACCTGGACATCATCTG-3'; reverse, 5'-CTGTTCCTTGGTCTGTGGTCTTTG-3'; Il1b, forward, 5'-AATCTCACAGCAGCATCTCGACAAG-3'; reverse, 5'-TCCACGGGCAAGACATAGGTAGC-3';  $\beta$ -actin, forward, 5'-TGTCACCAA CTGGGACGATA-3'; reverse, 5'-GGGGTGTGAAGGTC TCAA-3'.

### Statistical method

All results are presented as mean  $\pm$  standard deviation (S.D.) and analyzed using GraphPad Prism 9.0 software (GraphPad Software, La Jolla, California, USA). Comparisons between two groups are performed using an unpaired *t* test, with results expressed as mean  $\pm$  standard deviation and illustrated with bar graphs. A *p* value of less than 0.05 is considered statistically significant.

## Results

### Establishment of AOCS rat model and study of long flexor muscle mRNA expression

In each of the experimental and control groups, there were 3 rats (j1,2,3 for the experimental group, j4,5,6 for the control group). When the  $\Delta p$  of rats in the experimental group was  $< 30$  mmHg, and the duration was  $> 2$  h, AOCS was diagnosed, indicating the successful modeling (Fig. 2A). Toe flexor muscles from the hind legs of rats in the experimental and control groups were subjected to second-generation high-throughput sequencing. Initially, mRNA samples were analyzed, and correlation analysis showed high transcription specificity between different samples in both the experimental and control groups. In different mapping distributions, the mapping ratio of genes in different samples was consistently above 70% (Fig. 3A). In addition, sequencing depth was similar between different samples (Fig. 3B, C). Three-dimensional PCA analysis indicated a good clustering of samples from both the experimental and control groups. Gene expression difference analysis revealed that compared to the control group, the muscles in the

experimental group had 247 genes significantly downregulated and 415 genes significantly upregulated (Fig. 3D). Functional enrichment analysis indicated that the upregulated genes were primarily associated with inflammation, immune cell activation and migration, and immune chemotaxis-related processes (Fig. 3E, F), including genes, such as Il1b, Cxcl3, Cxcl2, Il6, Il1r2, and others. Specific to activated cell types and signaling pathways, infiltration and migration of neutrophils and enrichment of the MAPK signaling pathway, such as high expression of the fos gene, were observed. Hypoxic response was also a significant characteristic expression pattern, with genes like Edn1, Egr1, Hp, Il1b, Junb, Jund, Nos2 showing high expression in AOCS muscles. Furthermore, attention was drawn to programmed cell death, prominently positioned in the GO enrichment results, with related genes including Nod2, Homx1, and Slc39a14. Previous studies have suggested that Homx1 and Slc39a14 are involved in the regulation of iron death [20]. Protein–protein interaction analysis revealed that proteins encoded by upregulated genes in the AOCS group were mostly related to immune cells (Fig. 3G), such as the interaction of Ptpcr with other genes. Ptpcr serves as a specific marker protein for immune cells. In addition, protein Nfkbiz in the NF- $\kappa$ B signaling pathway interacts with IL33 receptor, as well as interactions between inflammatory chemokines Cxcl1/Cxcr2, collectively indicated that AOCS is an inflammatory disease involving the immune system.

### KEGG enrichment analysis of upregulated genes in the AOCS group

Based on the KEGG pathway analysis of upregulated genes in the AOCS group, we found that the predominantly enriched pathways were related to the immune system and signal transduction. In addition, metabolism and endocrine pathways also held significant positions (Fig. 4A). This suggests that the upregulated genes in AOCS may originate from the expression of immune cells, and their functions may involve signaling and functional activation of immune cells. Specifically in terms of signaling pathways, we observed that tuberculosis and other bacterial infections were among the top pathways (Fig. 4B), and the activation of the TNF signaling pathway and NF- $\kappa$ B signaling pathway was significant. The enrichment of cytokine–cytokine receptor interaction was the highest, consistent with the classification results of signaling transduction. Bacterial infection enrichment is generally associated with neutrophils. After neutrophils are activated, they release granule proteins and chromatin, which together form extracellular fibers that can bind to both Gram-positive and Gram-negative bacteria. These neutrophil extracellular traps (NETs) can degrade bacterial virulence factors and kill bacteria [21].

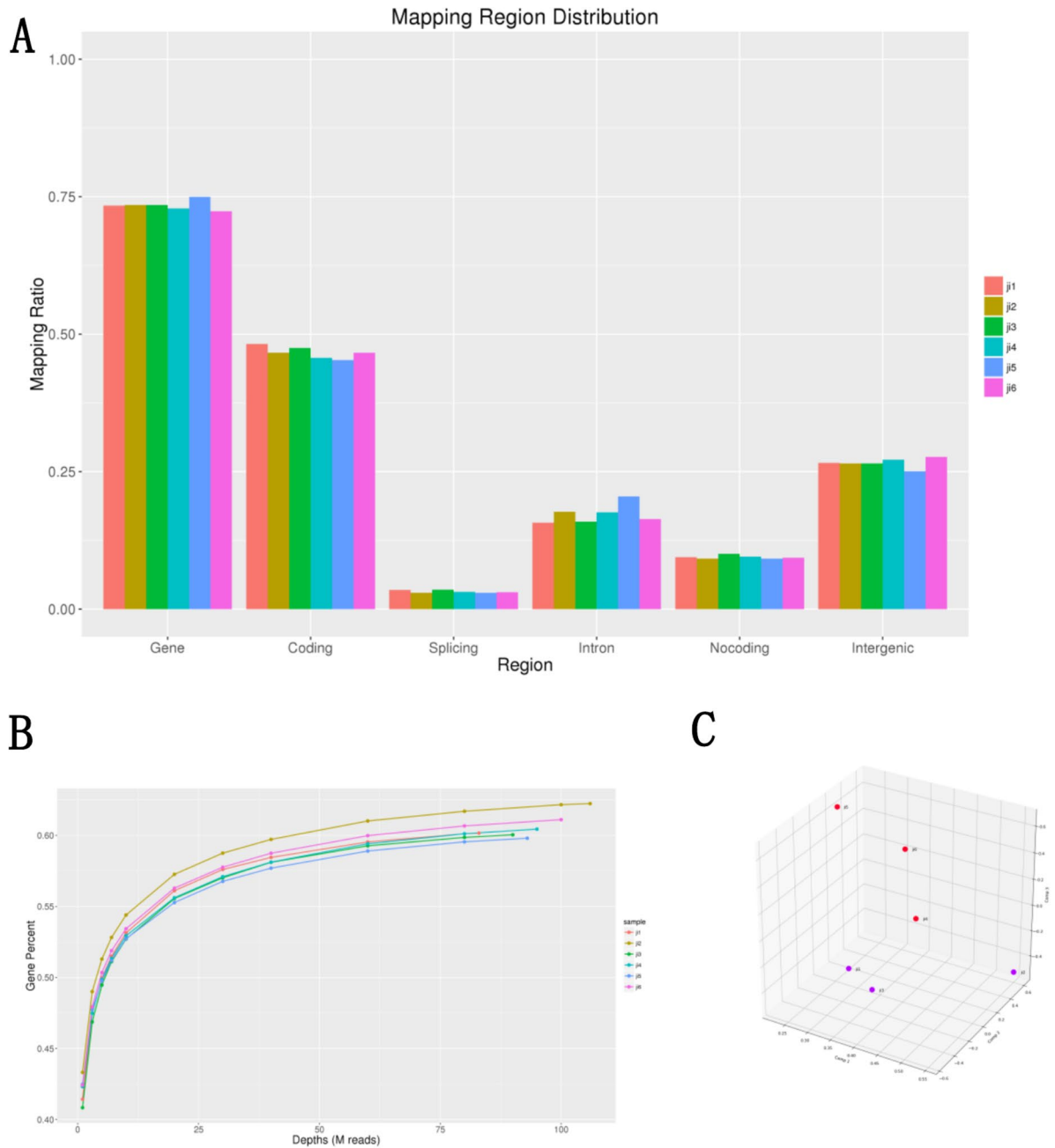


**Fig. 3** Differently expressed genes between AOCS groups and Ctrl groups (j1,2,3 for the experimental group, j4,5,6 for the control group). **A**, **B** Quality of mRNA expression sequence in the rat AOCS model. **C** PCA analysis of 6 samples for RNA seq data. **D** Heatmap showed the DEGs in AOCS groups compared with Ctrl groups: The branch tree on the left side of the heat map indicates the clustering of gene expression patterns, with genes with similar expressions grouped together; red indicates high gene expression  $\log_2\text{FoldChange} > 0$ , and green indicates low gene expression  $\log_2\text{FoldChange} < 0$ ; the branch tree at the top of the heat map indicates the clustering relationship between samples: j1, 2, 3 are experimental groups, and j4, 5, 6 are control groups. **E**, **F** GO enrichment analysis of upregulated in AOCS groups. **G** PPI analysis for upregulated genes in AOCS groups: the size of the node is proportional to the degree of interaction of the protein. The higher the degree of interaction, the larger the node, indicating that the protein is an important hub in the network; the connecting line indicates the direct interaction verified by the experiment

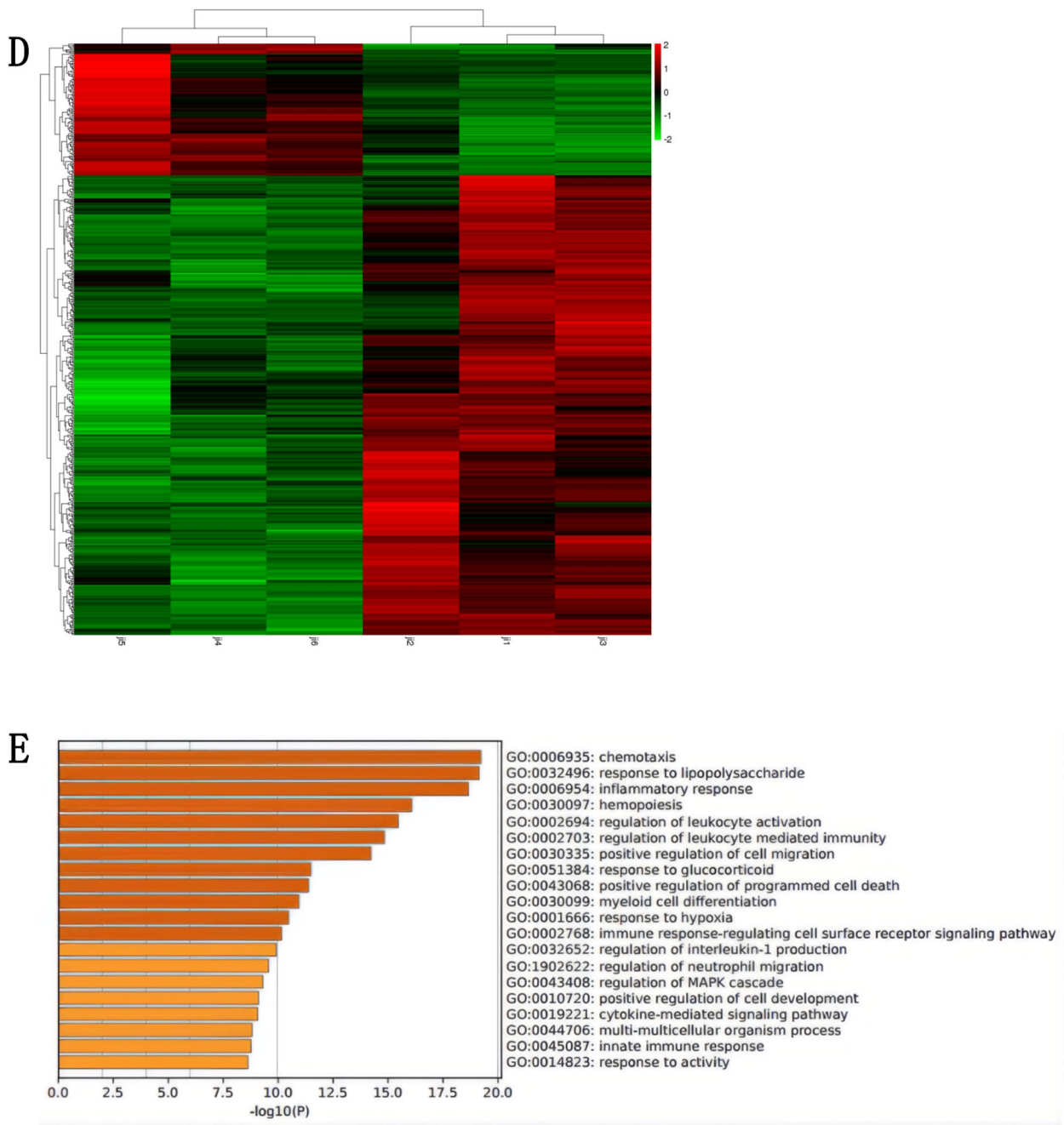


Fig. 3 continued

**Changes in the expression of lncRNA, circRNA, and miRNA in the AOCs group**

Although we have gained a lot of new knowledge from the differential expression analysis of mRNA, we hope to further analyze the pathogenesis of AOCs by delving into non-coding RNA. The central dogma is well known to us all, but traditional central dogma can no longer completely summarize the genetic rules as the

discovery of non-coding RNA continues. Investigating its functions has become imperative [22]. Eukaryotic genomes contain a large amount of non-coding DNA, even exceeding 97% in humans. In the past, these sequences were thought to have no function and were thus labeled as "junk" DNA. These "junk DNA" mainly includes introns, simple repeat sequences, mobile sequences, and their remnants.

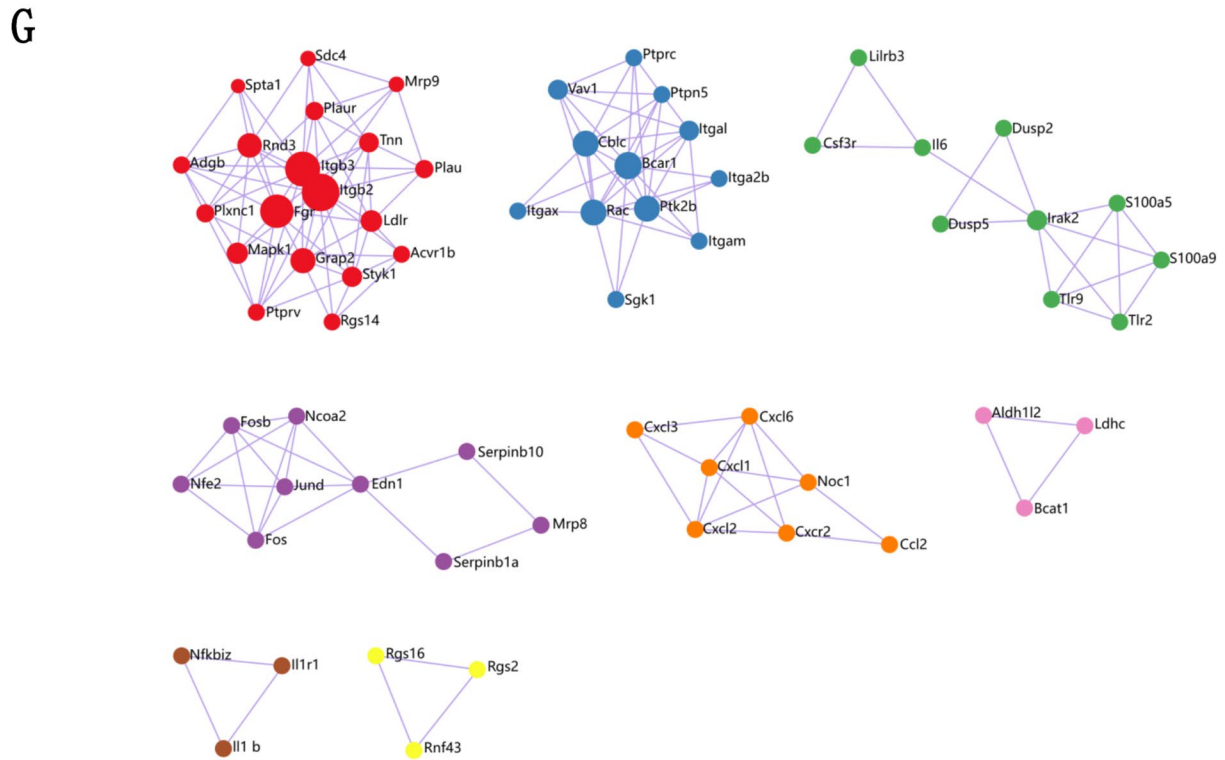
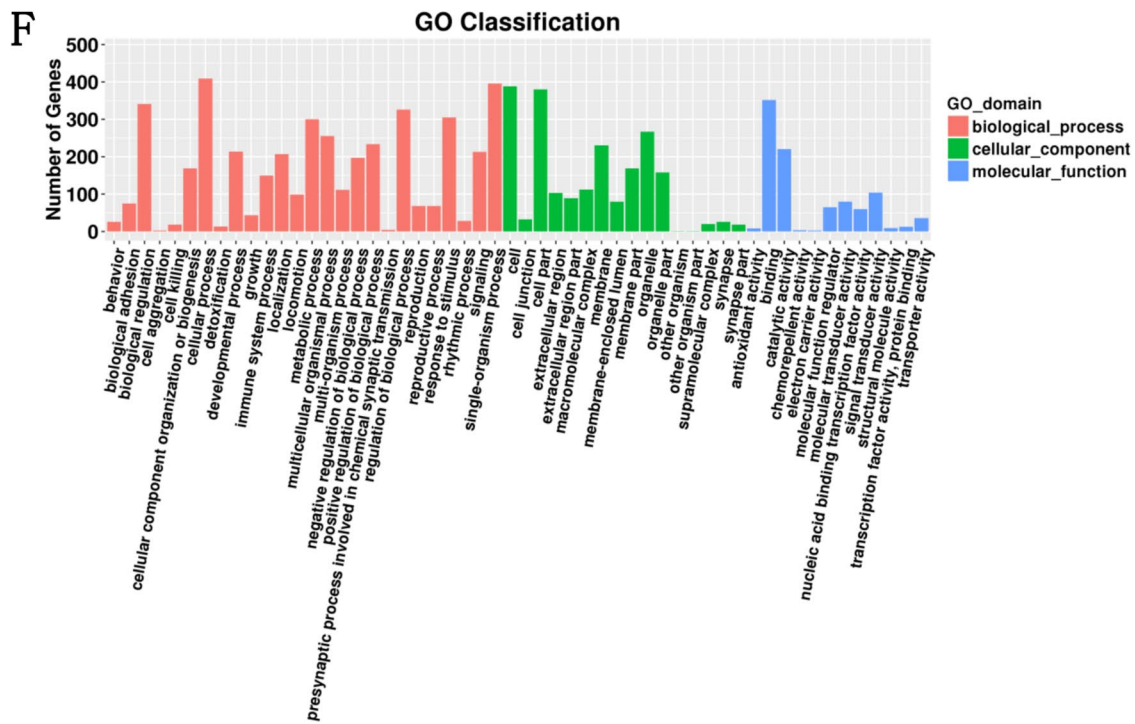


Fig. 3 continued



Research indicates that these DNA sequences that do not directly produce proteins play an equally important role in life activities. Most non-coding DNA plays an essential role in the effective activity of the corresponding genes. Common regulatory non-coding RNAs include MicroRNA, long non-coding RNA, and circular RNA [23–25].

First, we analyzed long non-coding RNA and found that lncRNA exhibited consistency with mRNA expression, with the ratio of transcripts tending to be consistent across different exons (Fig. 5A), suggesting that lncRNA may be involved in the expression regulation of these differentially expressed genes. Differential expression analysis revealed upregulation or downregulation of lncRNA in both the experimental and control groups (Fig. 5B). Based on database analysis, we predicted the genes that these differentially expressed lncRNAs might target. Functional enrichment analysis of these predicted genes showed that they are associated with biological processes, such as oxidative stress respiratory chain, secretion of inflammatory factor IL8, NK cell killing, and phospholipid catalysis (Fig. 5D). The analysis of lncRNA–mRNA interactions indicated that lncRNA interacts with the CD45 protein, participating in the regulation of immune cells, and is associated with genes in the MAPK signaling pathway, such as Junb (Fig. 5D).

Circular RNA is a type of non-coding RNA formed by reverse splicing of pre-mRNAs and is abundantly present. circRNAs share properties similar to lncRNAs, participating in transcription and translation regulation, and can function as "miRNA-sponges." Compared to the control group, differential circRNA can obtain parental gene information (Fig. 6A). The GO functional enrichment analysis of the parental gene of diff\_circRNA revealed associations with metal ion binding, cytoskeletal protein binding and assembly, and smooth muscle cell development, possibly related to stress responses in muscle cell inflammation (Fig. 6B). KEGG analysis suggested that these circRNAs may be associated with ubiquitin-mediated protein hydrolysis, cell engulfment, and metabolism (Fig. 6C).

miRNA downregulates the expression of target gene mRNA in the cytoplasm by binding to the seed region of the 3'-UTR, representing its classical biological function. Functional enrichment analysis of the predicted miRNA-targeted mRNAs differentially expressed in AOCS revealed associations with ankyrin binding and glycerol kinase activity (Fig. 6D). KEGG analysis indicated that these miRNAs may be associated with Wnt signaling, Vegf signaling, and MAPK signaling (Fig. 6E).

### mRNA–miRNA–lncRNA integrated analysis

To depict the complex biological processes during the onset of AOCS, we further conducted an integrated analysis of mRNA–miRNA–lncRNA (Fig. 7). We observed that iron-death-related genes, such as Slc39a14, and their family proteins like Slc4a1 and Slc7a8, are involved in interactions with non-coding RNAs, suggesting the involvement of iron death in the pathogenesis of AOCS. In addition, proteins related to the MAPK signaling pathway (dusp5), inflammation-related receptor (Ifnlr1), and transcription factor (runx3) showed interaction associations with miRNA–lncRNA, indicating potential regulatory functions of non-coding RNAs in the pathogenesis of AOCS.

### RT-qPCR analysis of gene expression in AOCS rat model

To further elucidate the expression profile of relevant genes, we performed real-time quantitative PCR (RT-qPCR). Our findings demonstrated that, compared to the control group, there was a significant upregulation of Edn1, Egr1, Hp, Il1b, Junb, Jund, Nos2, Nod2, Homx1, Slc39a14, Ptpcr, Nfkbiz, IL33, Cgas, Sting, Cxcl1, and Cxcr2 mRNA levels in the AOCS rat model (Fig. 8A). These results are consistent with second-generation high-throughput sequencing data, reinforcing the reliability of the sequencing outcomes and suggesting involvement in processes related to inflammation, hypoxia, immune cell activation and migration, and chemotaxis in AOCS. Conversely, a downregulation of Gpx4 mRNA suggests the occurrence of ferroptosis in AOCS (Fig. 8B).

### Discussion

Based on multi-omics sequencing of the rat AOCS model, we have identified AOCS as an inflammatory condition mediated by the immune system. In our functional enrichment analysis of sequencing data as well as through protein interaction analysis, we observed that the proteins encoded by the upregulated genes in the AOCS group were mainly associated with immune cells, and the upregulated genes were mainly related to inflammatory response and immune response, including genes, such as Edn1, Egr1, Hp, Il1b, Junb, Jund, Nos2, Nod2, Homx1, Slc39a14, Ptpcr, Nfkbiz, IL33, Cxcl1 and Cxcr2.

Recently, the cGAS–STING pathway has been extensively studied, gradually unveiling its role in regulating inflammatory responses and maintaining immune balance [26–29]. In the context of inflammatory diseases, the regulation of immune cell functions, such as those of macrophages and neutrophils, is crucial to disease progression [30, 31]. This study's findings show an

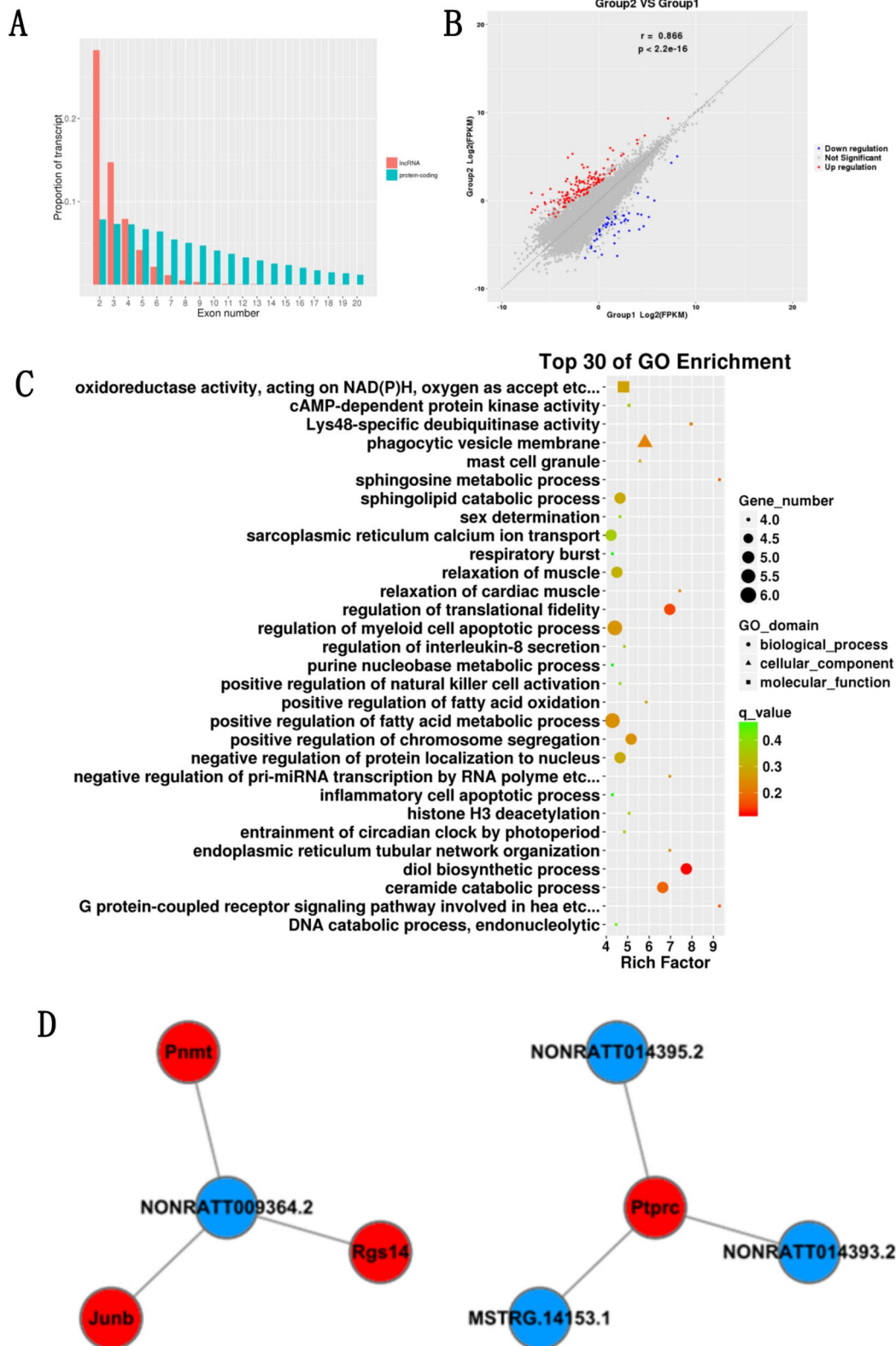


**Fig. 5** **A** Exon count distribution between lncRNA and mRNA. **B** Diff\_lncRNA between group 1 and group 2. **C** GO enrichment analysis for lncRNA targeted mRNAs(predicted). **D** diff\_mRNA and lncRNA co-expression

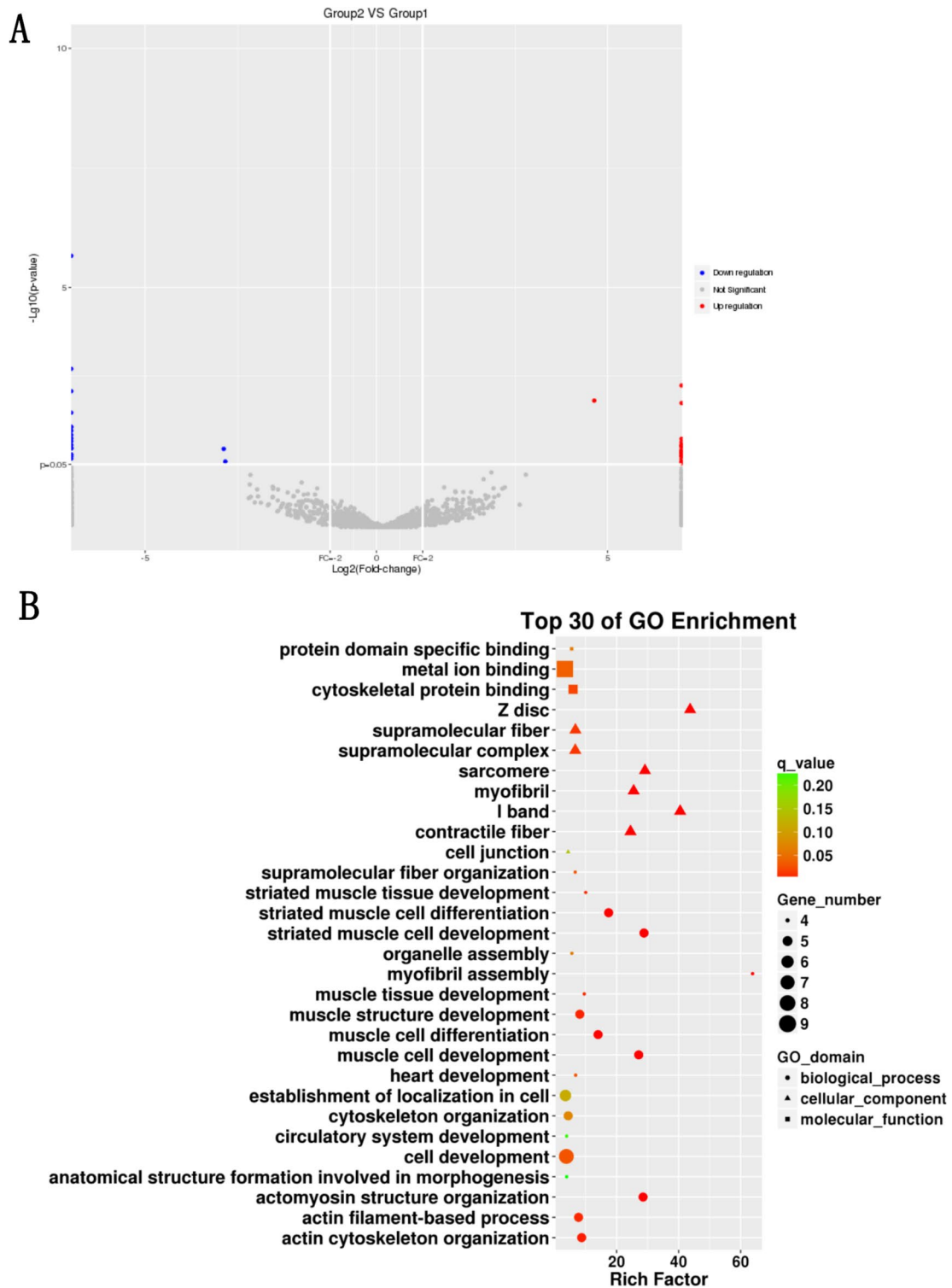


**Fig. 6** A–C circRNA GO, KEGG enrichment for diff\_circRNA parental gene. **D, E** GO enrichment analysis for miRNA targeted mRNAs (predicted)

enrichment of gene functions associated with neutrophil migration in AOCS, indicating Ptpcr, Nfkbiz, and IL-33 as key molecules regulating these immune cell functions.

Thus, we can reasonably infer that Ptpcr, Nfkbiz, and IL-33 may influence immune functionality and, consequently, inflammation and disease progression through

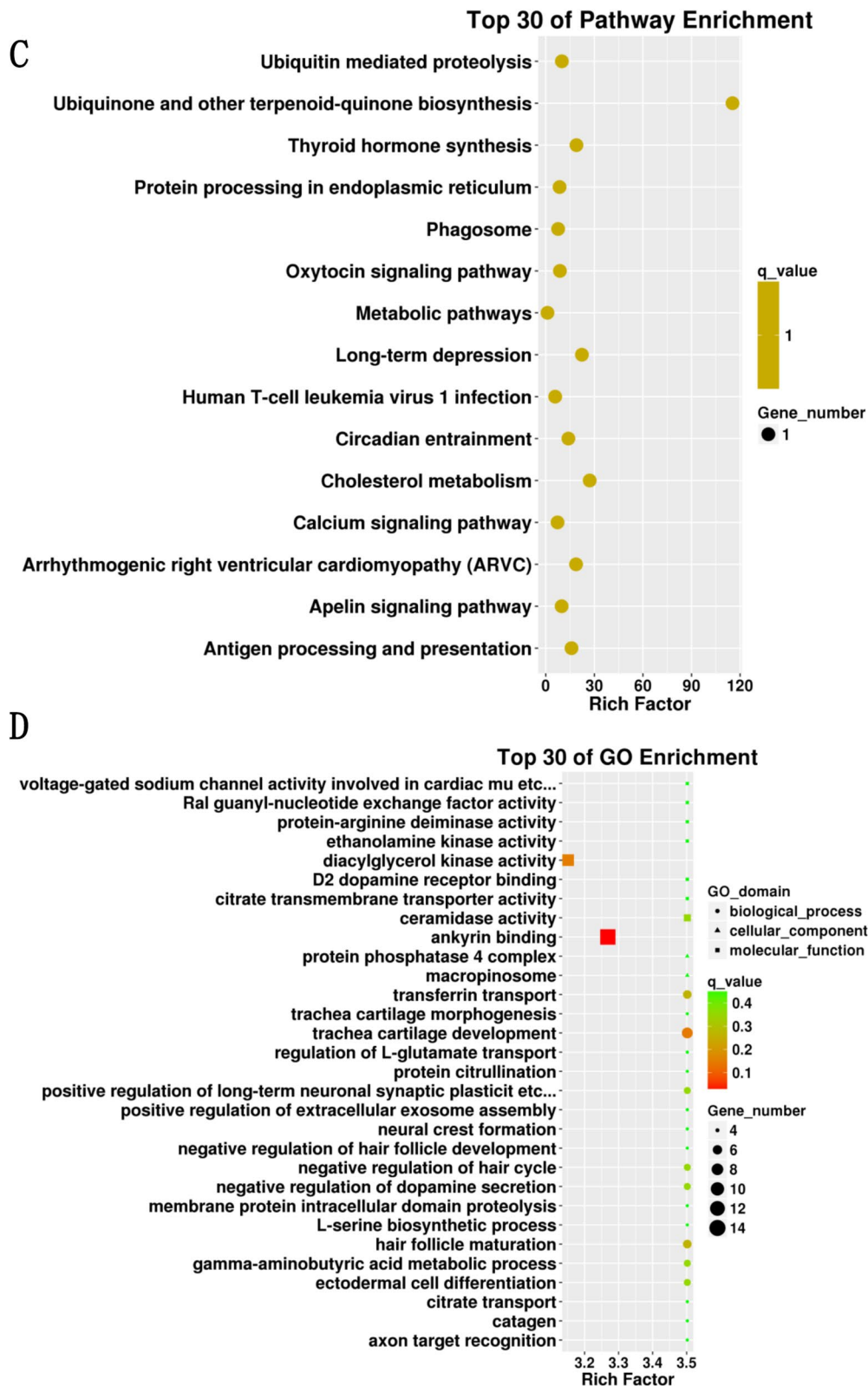


Fig. 6 continued

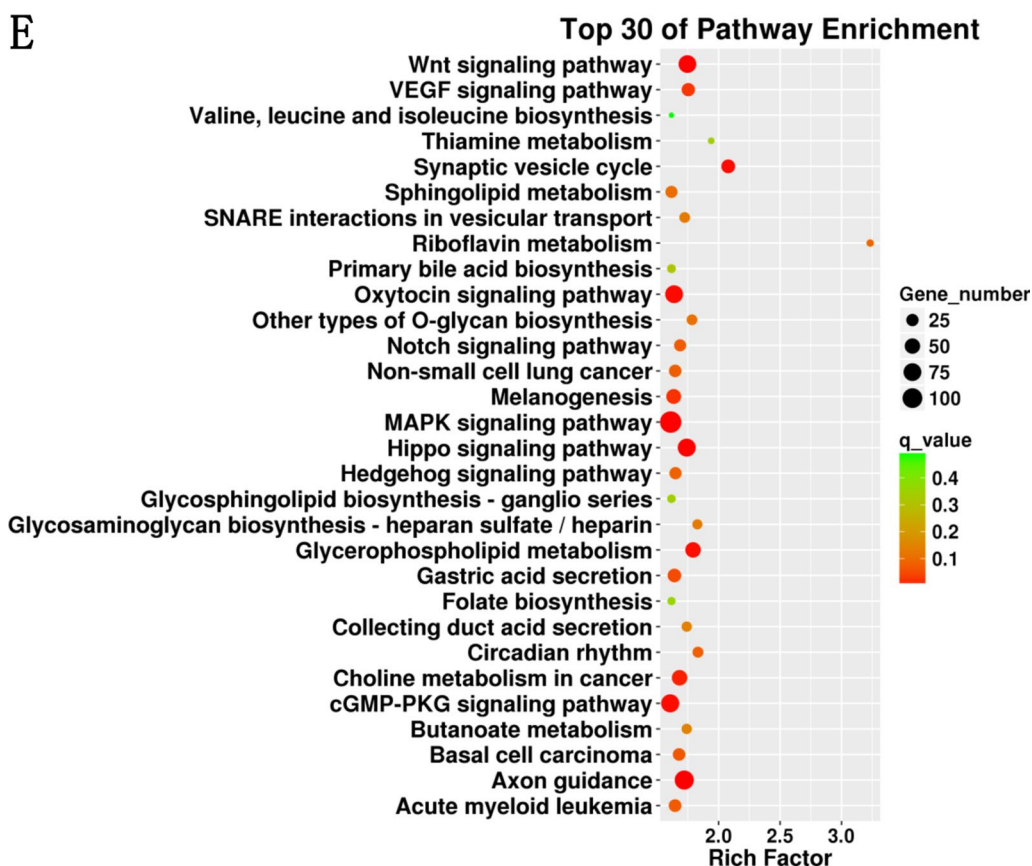


Fig. 6 continued

direct or indirect regulation of the cGAS–STING pathway. Ptpcr, a specific marker protein for immune cells and acting as a tyrosine phosphatase, is essential for T cell and B cell receptor signal transduction, regulating immune cell activation and function. Ptpcr finely tunes the intracellular signaling pathways of immune cells through the dephosphorylation of specific substrates, thereby affecting the immune response. The cGAS–STING pathway represents a critical intracellular DNA-sensing mechanism that, upon detecting abnormal DNA (such as DNA released during viral infection or cell damage), activates STING through the secondary messenger cGAMP, leading to the production of IFN $\beta$  and an inflammatory response [32]. This pathway plays a key role in defending against viral infections and regulating autoimmune responses [12]. Although the direct interaction between Ptpcr and the cGAS–STING pathway is not well-documented, it is plausible that Ptpcr could indirectly affect the cGAS–STING pathway’s activity by influencing the signaling environment within immune cells. It is believed that Ptpcr can regulate signaling pathways, such as JAK/STAT and MAPK, which are closely associated with downstream signaling of the

cGAS–STING pathway [33–35]. Accordingly, Ptpcr could affect the activity of downstream effectors like IRF3 and TBK1 in the cGAS–STING pathway, key molecules responsible for producing IFN $\beta$  and, thereby, influencing the release of IFN $\beta$  and inflammatory factors.

Moreover, it is worth noting that our study results show upregulated expression of Nfkbiz and IL-33 in the experimental group compared to the control group. Research indicates that the NF- $\kappa$ B signaling pathway is one of the key pathways regulating cell survival, inflammation, and immune responses [36]. By modulating the NF- $\kappa$ B pathway, Nfkbiz may indirectly impact the activation and function of the cGAS–STING pathway. IL-33 activates downstream signaling through binding with its specific receptor ST2, thereby activating NF- $\kappa$ B and MAPK signaling pathways, leading to inflammatory responses and Th2-type immune reactions [37]. Therefore, we speculate that Nfkbiz and IL-33 may indirectly affect the activity of the cGAS–STING pathway by affecting the signaling environment within immune cells. It is posited that the activation of the NF- $\kappa$ B pathway, by promoting the expression of inflammatory cytokines, chemokines, and interferon-stimulated genes (ISGs), could influence the



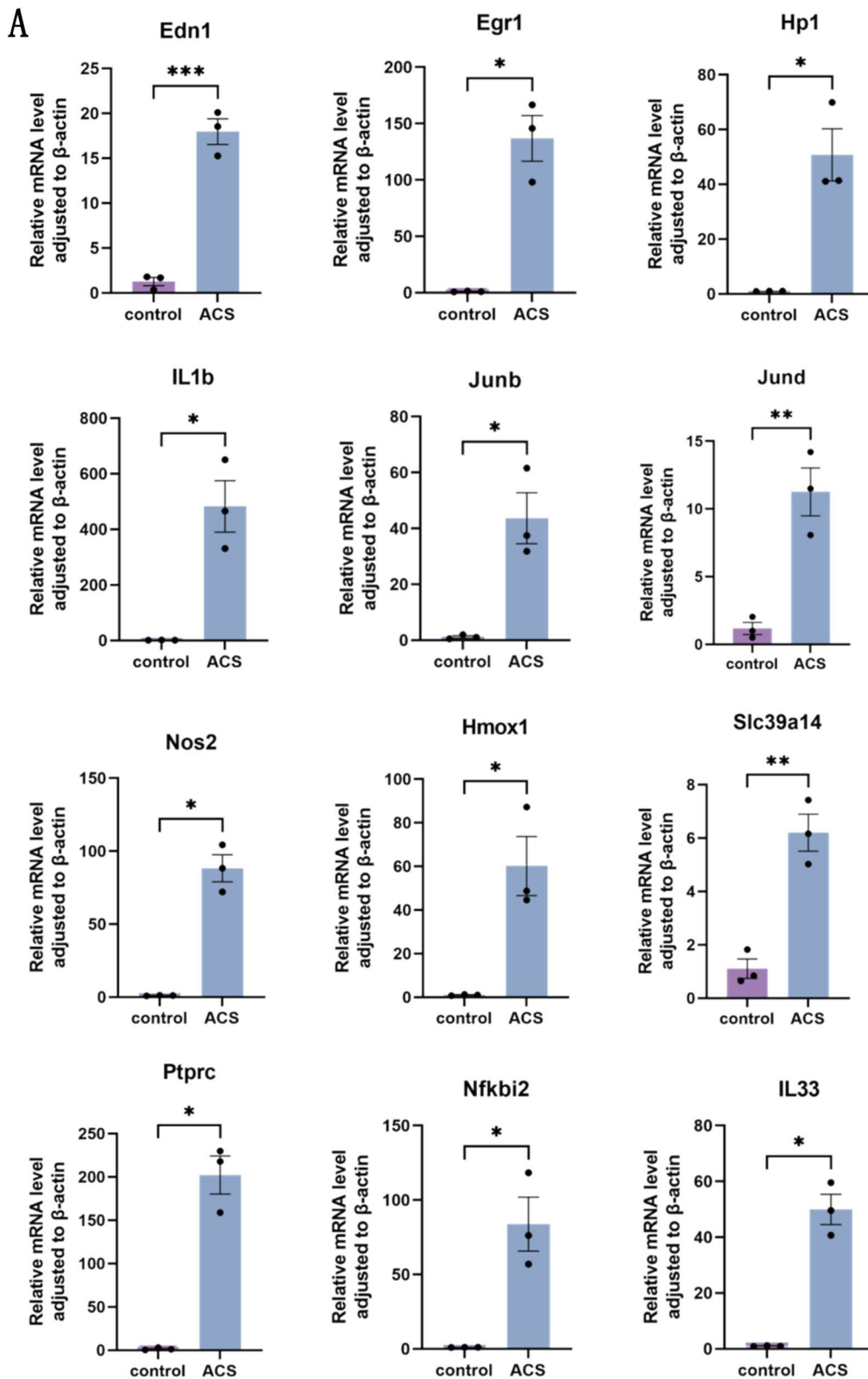


**Fig. 8 A, B** PCR analysis of related gene expression. Significance levels: \* $p < 0.05$ , \*\* $p < 0.01$ , \*\*\* $p < 0.001$ . **C** Mechanistic linkage of ferroptosis-related genes with cGAS–STING and NF- $\kappa$ B pathways

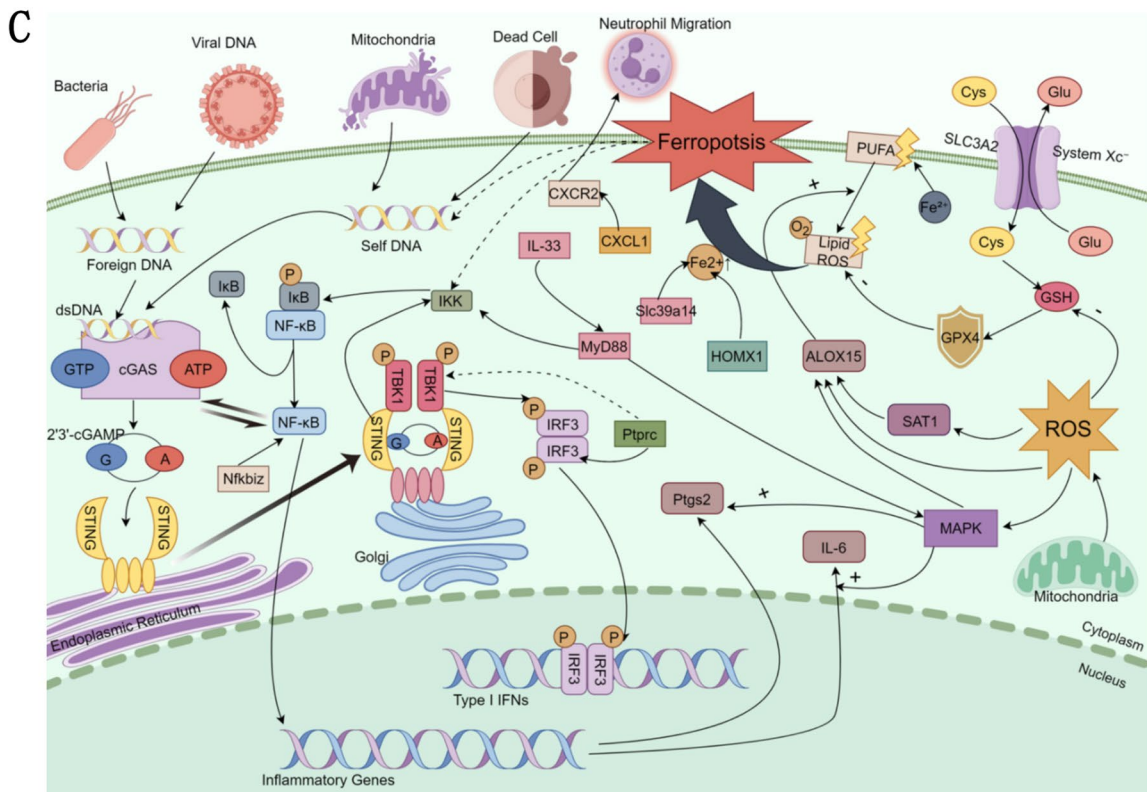
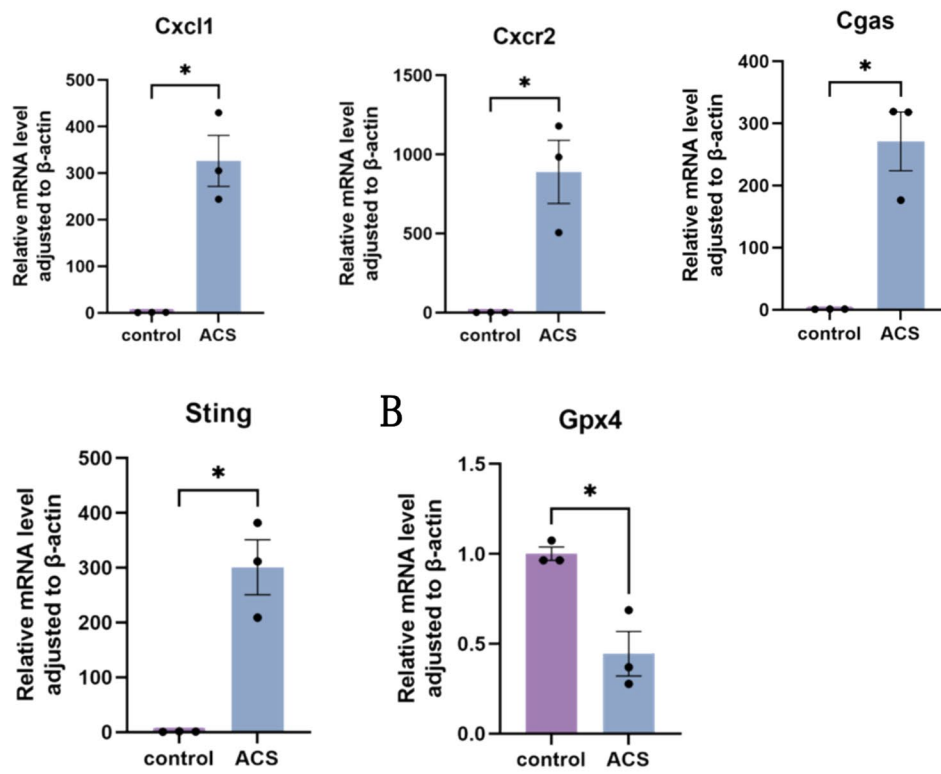


Fig. 8 continued

amount of ROS, further aggravating oxidative stress [41, 42]. The activation of the NF- $\kappa$ B pathway is closely related to the cell's response to DNA damage and stress. This response, by influencing the cell's DNA-sensing mechanisms like the activity of cGAS [43], indirectly modulates the activation of the cGAS–STING pathway. Nfkbiz and IL-33 may regulate the cell's response to stress and damage, indirectly impacting the cGAS–STING pathway's activation. The release of DAMPs (Damage-Associated Molecular Patterns) during cellular stress or damage could affect the activation state of the cGAS–STING pathway, modulating the immune cell response [44]. Overall, Nfkbiz and IL-33 play critical roles in the NF- $\kappa$ B signaling pathway, affecting immune responses through the regulation of inflammatory cytokine production and release, and play essential functions in the inflammatory environment of AOCS. Nfkbiz, by controlling NF- $\kappa$ B activity, influences the expression of inflammatory genes, regulating immune cell functionality and inflammation. In contrast, IL-33, as a pro-inflammatory cytokine, activates its receptor ST2 and further activates downstream signaling molecules like MyD88, IRAK, and TRAF6, ultimately activating the NF- $\kappa$ B and MAPK signaling pathways, promoting the production of inflammatory factors and Th2-type immune responses. In AOCS, the inflammatory response triggered by tissue injury activates the Nfkbiz and IL-33/ST2 axis, affecting the disease process by regulating post-injury inflammation and immune response. This mechanism may indirectly affect the activation state of the cGAS–STING pathway by regulating the release of DAMPs. DAMPs, as critical factors in activating the cGAS–STING pathway [45], may regulate immune cell responses, including the production of IFN $\gamma$  and inflammatory factors, thereby further affecting inflammation and immune regulation in AOCS. This suggests that the regulatory effects of Nfkbiz and IL-33/ST2 axis through the NF- $\kappa$ B pathway may be closely related to the cGAS–STING pathway, providing a new perspective for understanding the interaction of signaling pathways in inflammation and immune function (Fig. 8).

Moreover, this study showed that the expression of Cxcl1 and Cxcr2 in the experimental group was higher than that in the control group. The chemokine Cxcl1 and its receptor Cxcr2 play a key role in the migration and activation of immune cells, such as neutrophils, significantly affecting local and systemic inflammatory responses [46]. These chemokines further exacerbate inflammation by attracting immune cells to sites of inflammation or injury. As an important mechanism for sensing abnormal intracellular DNA, the cGAS–STING pathway can enhance pathogen defense and regulate immune responses by activating the release of IFN $\gamma$  and inflammatory factors. In AOCS, tissue damage

and DAMP release caused by ischemia may activate the cGAS–STING pathway, promote the production of IFN $\gamma$  and inflammatory mediators, and trigger the aggregation and activation of more immune cells. At the same time, the activation of the Cxcl1/Cxcr2 axis enhances the migration of neutrophils to damaged areas and exacerbates the inflammatory response. This suggests that the two pathways may interact in AOCS-related inflammation and jointly regulate the intensity and duration of immune responses and inflammation. Although direct evidence is limited, these mechanisms are consistent with our findings, revealing the important interaction between the Cxcl1/Cxcr2 axis and the cGAS–STING pathway in the inflammatory environment of AOCS, which has a profound impact on the course of the disease.

During the functional enrichment analysis of upregulated genes in the inflammatory process, a significant involvement of programmed cell death was observed. Notably, Homx1 and Slc39a14 were identified as participants in the regulation of iron death, suggesting the potential involvement of the iron death process in the pathogenesis of AOCS. In AOCS samples, Slc39a14 showed high expression. Slc39a14 belongs to the SLC39/ZIP family and functions as a transmembrane protein involved in the transport of a broad spectrum of metal ions, mediating cellular uptake of ions [47]. Among the SLC39 family members, SLC39A14 is implicated in regulating iron death. Conditional knockout of SLC39A14 significantly reduced liver absorption of NTBI (non-transferrin-bound iron) and prevented liver iron overload in a hemochromatosis mouse model [48]. In addition, conditional knockout of SLC39A14 reduced iron accumulation in the liver and iron death-mediated liver fibrosis, indicating that SLC39A14-mediated iron uptake promotes iron death-induced liver injury and disease [49].

Furthermore, we observed that differentially expressed genes were frequently enriched in bacterial infections, including *Mycobacterium tuberculosis* infection. Within the immune system, neutrophils, a major cell type involved in antibacterial responses, were highlighted [50]. The functional enrichment results of upregulated genes in AOCS also indicated the migration of neutrophils. This led us to reasonably infer that neutrophils are the primary immune cell type involved in AOCS disease. Interestingly, previous research has suggested a close association between neutrophil iron death and the onset of systemic lupus erythematosus (SLE). It has been elucidated that neutrophil iron death in SLE patients is induced by the synergistic action of autoantibodies and IFN- $\alpha$ , promoting the binding of the transcriptional repressor CREM $\alpha$  to the GPX4 promoter, thereby downregulating GPX4 protein expression. In vivo studies found that specific

myeloid cell Gpx4 knockout mice exhibit clinical manifestations similar to SLE. Administering the iron death inhibitor liproxstatin-1 to these model mice can alleviate SLE symptoms and mitigate the progression of the disease [51]. In our AOCS model study, the evidence supports a similar mechanism, suggesting that neutrophils may upregulate Homx1 and Slc39a14, leading to iron death and exacerbating inflammation.

The clinical implications of this study are significant. Identifying ferroptosis and cGAS–STING pathway components as key contributors to AOCS provides actionable insights for therapeutic development. For instance, ferroptosis inhibitors could reduce tissue damage, while cGAS–STING pathway modulators might mitigate excessive immune activation. Moreover, the upregulated genes identified, such as Slc39a14 and Ptpcr, could serve as biomarkers for early diagnosis or disease progression monitoring, facilitating timely interventions. By elucidating the molecular underpinnings of AOCS, this study bridges the gap between basic research and clinical applications, offering new avenues for improving patient outcomes.

### Limitations and future

**Directions** Despite its contributions, this study has limitations that warrant consideration. The use of a rat model, while informative, may not fully capture the complexity of human AOCS. In addition, the small sample size limits the generalizability of the findings. The reliance on multi-omics data, though comprehensive, necessitates further validation through functional experiments and clinical studies to confirm the identified pathways' roles in AOCS pathogenesis. Future research should explore the interplay between ferroptosis, cGAS–STING signaling, and oxidative stress in greater depth, with a focus on translating these findings into effective therapies. Expanding sample diversity and incorporating human tissue studies will be critical for validating the translational potential of these discoveries.

This study underscores the interplay between immune pathways, oxidative stress, and ferroptosis in AOCS pathogenesis. Addressing these mechanisms through targeted interventions could significantly improve treatment outcomes, providing a foundation for future translational research.

### Conclusions

In summary, our multi-omics analysis of mRNA, lncRNA, circRNA, and miRNA sequencing data provides insights into the pathogenesis of AOCS. We discovered that AOCS constitutes a complex, immune-mediated inflammatory disease, characterized by intricate interactions among mRNA, lncRNA, and circRNA, actively

participating in immune regulation. Neutrophils emerge as the primary immune cells, while genes associated with ferroptosis are highly expressed in the model, with non-coding RNAs involved in their synergistic regulation. These findings suggest that neutrophils may undergo ferroptosis, thereby amplifying the inflammatory response in the fascial compartments and promoting disease progression. Simultaneously, this study reveals how immune molecules and pathways interact within AOCS, bearing significant implications for deeper understanding of the AOCS disease mechanism and the development of targeted therapeutic strategies.

### Acknowledgements

We thank everyone involved for their efforts in the writing and critical review of this manuscript.

### Author contributions

ZH and SW designed this study. QZL and HL are responsible for writing articles, conducting statistical analysis, reviewing articles, and creating images. QZL, YHL and JLL are responsible for collecting data and conducting statistical analysis.

### Funding

This work was supported by the Guangxi Natural Science Foundation (2019GXNSFAA245065), the Guangxi Science and Technology Base and Talent Special Project (GuikeAD20159024), Guangxi Key research and development program (AB19110017). The authors, therefore, acknowledge with thanks their technical and financial support.

### Availability of data and materials

No datasets were generated or analysed during the current study.

### Declarations

#### Ethics approval and consent to participate

This study was approved by the First Affiliated Hospital of Guangxi Medical University Ethics Review Committee (2023-E716-01). Exemption of informed consent from patients with the consent of the ethics committee. In our experiment, we strictly adhere to the principle of humane endpoints to ensure that animals receive prompt and humane treatment whenever any pain or distress occurs. All experimental procedures are carried out with the principle of minimizing animal suffering to the greatest extent.

#### Consent for publication

All authors have read and approved the final manuscript. We confirm that we have obtained consent from all participants involved in the study for their data to be published.

#### Competing interests

The authors declare no competing interests.

Received: 20 November 2024 Accepted: 9 January 2025

Published online: 05 February 2025

### References

1. Von Keudell AG, Weaver MJ, Appleton PT, et al. Diagnosis and treatment of acute extremity compartment syndrome. *Lancet*. 2015;386(10000):1299–310.
2. McQueen MM, Gaston P, Court-Brown CM. Acute compartment syndrome. Who is at risk? *J Bone Joint Surg British*. 2000;82(2):200–3.
3. Schmidt AH. Acute compartment syndrome. *Injury*. 2017;48(Suppl 1):S22–5.

4. Long B, Koifman A, Gottlieb M. Evaluation and management of acute compartment syndrome in the emergency department. *J Emerg Med.* 2019;56(4):386–97.
5. Cone J, Inaba K. Lower extremity compartment syndrome. *Trauma Surg Acute Care Open.* 2017;2(1):e000094.
6. Glass GE, Staruch RM, Simmons J, et al. Managing missed lower extremity compartment syndrome in the physiologically stable patient: a systematic review and lessons from a Level I trauma center. *Journal Trauma Acute Care Surg.* 2016;81(2):380–7.
7. Grechenig C, Valsamis EM, Koutp A, et al. Dual-incision minimally invasive fasciotomy of the anterior and peroneal compartments for chronic exertional compartment syndrome of the lower leg. *Sci Rep.* 2020;10(1):18113.
8. Kono H, Fujii H, Asakawa M, et al. Protective effects of medium-chain triglycerides on the liver and gut in rats administered endotoxin. *Ann Surg.* 2003;237(2):246–55.
9. Mañé J, Pedrosa E, Lorén V, et al. Partial replacement of dietary (n-6) fatty acids with medium-chain triglycerides decreases the incidence of spontaneous colitis in interleukin-10-deficient mice. *J Nutr.* 2009;139(3):603–10.
10. Orton RJ, Gu Q, Hughes J, et al. Bioinformatics tools for analysing viral genomic data. *Rev Sci Tech.* 2016;35(1):271–85.
11. Chen J, Coppola G. Bioinformatics and genomic databases. *Handb Clin Neurol.* 2018;147:75–92.
12. Xu Y, Chen C, Liao Z, et al. cGAS-STING signaling in cell death: mechanisms of action and implications in pathologies. *Eur J Immunol.* 2023;53(9):e2350386.
13. Tian M, Li F, Pei H, et al. The role of the cGAS-STING pathway in chronic pulmonary inflammatory diseases. *Front Med.* 2024;11:1436091.
14. Wan D, Jiang W, Hao J. Research advances in how the cGAS-STING pathway controls the cellular inflammatory response. *Front Immunol.* 2020;11:615.
15. Lawendy AR, Sanders DW, Bihari A, et al. Compartment syndrome-induced microvascular dysfunction: an experimental rodent model. *Can J Surg J Can de Chirurgie.* 2011;54(3):194–200.
16. Manjoo A, Sanders D, Lawendy A, et al. Indomethacin reduces cell damage: shedding new light on compartment syndrome. *J Orthop Trauma.* 2010;24(9):526–9.
17. Robinson MD, McCarthy DJ, Smyth GK. edgeR: a Bioconductor package for differential expression analysis of digital gene expression data. *Bioinformatics.* 2010;26(1):139–40.
18. Szklarczyk D, Franceschini A, Wyder S, et al. STRING v10: protein-protein interaction networks, integrated over the tree of life. *Nucleic Acids Res.* 2015;43:D447–52.
19. Shannon P, Markiel A, Ozier O, et al. Cytoscape: a software environment for integrated models of biomolecular interaction networks. *Genome Res.* 2003;13(11):2498–504.
20. Yan Q, Zheng W, Jiang Y, et al. Transcriptomic reveals the ferroptosis features of host response in a mouse model of Zika virus infection. *J Med Virol.* 2023;95(1):e28386.
21. Brinkmann V, Reichard U, Goosmann C, et al. Neutrophil extracellular traps kill bacteria. *Science.* 2004;303(5663):1532–5.
22. Panni S, Lovering RC, Porras P, et al. Non-coding RNA regulatory networks. *Biochim Biophys Acta.* 2020;1863(6):194417.
23. Lu TX, Rothenberg ME. MicroRNA. *J Allergy Clin Immunol.* 2018;141(4):1202–7.
24. Bridges MC, Daulagala AC, Kourtidis A. LNCcation: lncRNA localization and function. *J Cell Biol.* 2021;220(2).
25. Chen L, Wang C, Sun H, et al. The bioinformatics toolbox for circRNA discovery and analysis. *Brief Bioinform.* 2021;22(2):1706–28.
26. Elahi R, Hozhabri S, Moradi A, et al. Targeting the cGAS-STING pathway as an inflammatory crossroad in coronavirus disease 2019 (COVID-19). *Immunopharmacol Immunotoxicol.* 2023;45(6):639–49.
27. Hu B, Ma JX, Duerfeldt AS. The cGAS-STING pathway in diabetic retinopathy and age-related macular degeneration. *Future Med Chem.* 2023;15(8):717–29.
28. Maekawa H, Fain ME, Wasano K. Pathophysiological roles of the cGAS-STING inflammatory pathway. *Physiology.* 2023;38(4):0.
29. Wan X, Tian J, Hao P, et al. The cGAS-STING pathway: a ubiquitous checkpoint perturbing myocardial attributes. *Curr Vasc Pharmacol.* 2023;21(3):152–62.
30. Prame Kumar K, Nicholls AJ, Wong CHY. Partners in crime: neutrophils and monocytes/macrophages in inflammation and disease. *Cell Tissue Res.* 2018;371(3):551–65.
31. Hong C, Lu H, Huang X, et al. Neutrophils as regulators of macrophage-induced inflammation in a setting of allogeneic bone marrow transplantation. *Stem Cell Rep.* 2022;17(7):1561–75.
32. Fritsch LE, Kelly C, Pickrell AM. The role of STING signaling in central nervous system infection and neuroinflammatory disease. *WIREs Mech Dis.* 2023;15(3):e1597.
33. Irie-Sasaki J, Sasaki T, Penninger JM. CD45 regulated signaling pathways. *Curr Top Med Chem.* 2003;3(7):783–96.
34. Irie-Sasaki J, Sasaki T, Matsumoto W, et al. CD45 is a JAK phosphatase and negatively regulates cytokine receptor signalling. *Nature.* 2001;409(6818):349–54.
35. Wang Y, Luo J, Alu A, et al. cGAS-STING pathway in cancer biotherapy. *Mol Cancer.* 2020;19(1):136.
36. Barnabei L, Laplantine E, Mbongo W, et al. NF- $\kappa$ B: At the Borders of Autoimmunity and Inflammation. *Front Immunol.* 2021;12:716469.
37. Yi XM, Lian H, Li S. Signaling and functions of interleukin-33 in immune regulation and diseases. *Cell Insight.* 2022;1(4):100042.
38. Chen LY, Pang XY, Chen C, et al. NF- $\kappa$ B regulates the expression of STING via alternative promoter usage. *Life Sci.* 2023;314:121336.
39. Chouchani ET, Pell VR, James AM, et al. A unifying mechanism for mitochondrial superoxide production during ischemia-reperfusion injury. *Cell Metab.* 2016;23(2):254–63.
40. Madungwe NB, Zilberstein NF, Feng Y, et al. Critical role of mitochondrial ROS is dependent on their site of production on the electron transport chain in ischemic heart. *Am J Cardiovasc Dis.* 2016;6(3):93–108.
41. Tang SP, Mao XL, Chen YH, et al. Reactive oxygen species induce fatty liver and ischemia-reperfusion injury by promoting inflammation and cell death. *Front Immunol.* 2022;13:870239.
42. Ben Mkaddem S, Pedruzzi E, Werts C, et al. Heat shock protein gp96 and NAD(P)H oxidase 4 play key roles in Toll-like receptor 4-activated apoptosis during renal ischemia/reperfusion injury. *Cell Death Differ.* 2010;17(9):1474–85.
43. Gulen MF, Samson N, Keller A, et al. cGAS-STING drives ageing-related inflammation and neurodegeneration. *Nature.* 2023;620(7973):374–80.
44. Vasiyani H, Wadhwa B, Singh R. Regulation of cGAS-STING signalling in cancer: approach for combination therapy. *Biochim Biophys Acta.* 2023;1878(3):188896.
45. Yu H, Liao K, Hu Y, et al. Role of the cGAS-STING pathway in aging-related endothelial dysfunction. *Aging Dis.* 2022;13(6):1901–18.
46. Sawant KV, Sepuru KM, Lowry E, et al. Neutrophil recruitment by chemokines Cxcl1/KC and Cxcl2/MIP2: Role of Cxcr2 activation and glycosaminoglycan interactions. *J Leukoc Biol.* 2021;109(4):777–91.
47. Girijashanker K, He L, Soleimani M, et al. Slc39a14 gene encodes ZIP14, a metal/bicarbonate symporter: similarities to the ZIP8 transporter. *Mol Pharmacol.* 2008;73(5):1413–23.
48. Jenkitkasemwong S, Wang CY, Coffey R, et al. SLC39A14 is required for the development of hepatocellular iron overload in murine models of hereditary hemochromatosis. *Cell Metab.* 2015;22(1):138–50.
49. Yu Y, Jiang L, Wang H, et al. Hepatic transferrin plays a role in systemic iron homeostasis and liver ferroptosis. *Blood.* 2020;136(6):726–39.
50. Toller-Kawahisa JE, O'Neill LAJ. How neutrophil metabolism affects bacterial killing. *Open Biol.* 2022;12(11):220248.
51. Li P, Jiang M, Li K, et al. Glutathione peroxidase 4-regulated neutrophil ferroptosis induces systemic autoimmunity. *Nat Immunol.* 2021;22(9):1107–17.

## Publisher's Note

Springer Nature remains neutral with regard to jurisdictional claims in published maps and institutional affiliations.